

## **Development of glycosynthase with broad glycan specificity for the efficient glyco-remodeling of antibodies**

Sachin S Shivatare,<sup>a</sup> Lin-Ya Huang,<sup>a</sup> Yi-Fang Zeng,<sup>a</sup> Jung-Yu Liao,<sup>a</sup> Tsai-Hong You,<sup>a</sup> Shi-Yun Wang,<sup>a</sup> Ting Cheng,<sup>b</sup> Chih-Wei Chiu,<sup>a</sup> Ping Chao,<sup>a</sup> Li-Tzu Chen,<sup>a</sup> Tsung-I Tsai,<sup>c</sup> Chiu-Chen Huang,<sup>a</sup> Chung-Yi Wu,<sup>\*b</sup> Nan-Horng Lin,<sup>\*a</sup> and Chi-Huey Wong,<sup>\*b,c</sup>

<sup>a</sup>CHO Pharma Inc., Park Street, Nangang District, Taipei-11503, Taiwan.

E-mail: nhlin@chopharma.edu.tw

<sup>b</sup>Genomics Research Center, Academia Sinica, 128 Academia Road, Section 2, Nankang, Taipei 115, Taiwan.

E-mail: cyiwu@gate.sinica.edu.tw or chwong@gate.sinica.edu.tw

<sup>c</sup>Department of Chemistry, The Scripps Research Institute, 10550 North Torrey Pines Road, La Jolla, California 92037.

## Table of Content

1. Materials.....	S3
2. General Methods.....	S4
3. Generation of EndoS2 mutants.....	S6
4. The glycan hydrolytic activity of EndoS2 mutants.....	S7
5. Chemo-enzymatic synthesis of N-linked glycans.....	S8
6. The transglycosylation potential of EndoS2 and its mutants.....	S18
7. Transglycosylation of GlcNAc-Rituximab with various glycan oxazoline using EndoS2 mutants.....	S19
8. Preparation of diverse Rituximab variants.....	S22
9. Binding of the Glycoengineered Rituximab to the Stimulatory Fc $\gamma$ Receptor (Fc $\gamma$ RIIIa).....	S27
10. ADCC activity of glycoengineered anti-CD20 antibodies.....	S28
11. References.....	S30
12. Spectral data.....	S31

## 1 Materials

Monoclonal antibody Rituximab were products from Genentech Inc., (South San Francisco, CA). The endo-glycosidases EndoF1, EndoS2, and the  $\alpha$ -L-fucosidase cloned from *Bacteroides fragilis* NCTC 9343 were obtained according to our previous report.<sup>1</sup> The functional domain of  $\alpha$ -2, 3 sialyltransferase (JTFAJ-16)<sup>2</sup> and  $\alpha$ -2,6 sialyltransferase (JT-ISH-224)<sup>3</sup> were reported previously.<sup>4</sup> The recombinant enzymes used in this work including pyruvate kinase (PK), pyrophosphatase (PPA), cytidine monophosphate kinase (CMK), and CMP-sialic acid synthetases (CSS) are expressed and purified in our laboratory. Enzymatic reactions with cofactor regeneration were carried out according to the procedure reported previously from our group.<sup>5</sup>

.....

## 2 General Methods

### I) Site-directed Mutagenesis and Expression and Purification of Recombinant EndoS2.

The EndoS2 encoding gene, *ndoS2*, from *Streptococcus pyogenes* GAS NZ131 was synthesized and subcloned into the pET28a expression vector. The signal peptide sequence (amino acid 1-36) of *ndoS2* was replaced by a His<sub>6</sub>-tag on its N-terminal. The mutants of *ndoS2* were generated by site-directed mutagenesis according to the manufacturer's instructions (Agilent Technologies) that PCR reactions were performed by using *ndoS2* expression vector as a template and oligonucleotide pairs containing desired mutation as primers. Then, the amplified DNA was treated with DpnI and transformed into DH5 $\alpha$  competent cells. The mutated sequences were confirmed by DNA sequencing (Genomics). After the transformation into BL21 (DE3) competent cells for expression, cells were induced with 0.1 mM isopropyl- $\beta$ -D-thiogalactopyranoside (IPTG), the recombinant EndoS2 mutant proteins with their His<sub>6</sub> tag were expressed at 20°C for 16 h and pelleted by centrifugation at 6500 rpm for 30 min. The cells were resuspended in lysis buffer (30 mM HEPES, pH 8.0, 300 mM NaCl) and disrupted using Ultrasonic Processor (10 min, 4s-on/ 5s-off, ChromTech). The total cell lysates were centrifuged at 10000 rpm for 45 min and the soluble recombinant EndoS2 and mutant proteins were purified by immobilized metal-ion chromatography with a Ni-NTA column (GE Healthcare). The eluted protein fractions were collected and concentrated against storage buffer (30 mM HEPES, pH 8.0, 100 mM NaCl) by using Amicon ultra centrifugal filters 10 kDa. Concentrated protein samples were analyzed by SDS-PAGE, and protein concentration was quantified using a Nano-Drop 2000c spectrophotometer. The yield of production of the wild-type EndoS2 was approximately 35 mg/L, and the yield for the mutants (Fig. S1) was approximately 25 mg/L.

## **II) Preparation of GlcNAc-Rituximab from commercially available Rituximab.**

GlcNAc-Rituximab was produced from commercial Rituximab according to known protocols.<sup>1</sup>

## **III) Preparation of (Fuc $\alpha$ 1, 6) GlcNAc-rituximab.**

(Fuc $\alpha$ 1, 6) GlcNAc-rituximab was prepared according to known methods.<sup>6</sup>

## **IV) Intact protein mass analysis of glycoengineered mAb.**

For the intact protein mass analysis, an experiment was performed on a reverse phase LC ESI-Q/TOF system (Waters). C4 column was used to separate IgG sample at 60 °C by a linear LC gradient with mobile phases, buffer A: 0.1% formic acid (FA) and buffer B: 0.1 FA in acetonitrile at 0.4 mL/min flow rate. Mass range was set as 700-4000 for raw data acquisition and was further processed into molecule mass by using the MaxEnt1 function of Masslynx software.

.....

### 3 Generation of EndoS2 mutants.

EndoS2 shares 37% sequence identity with EndoS, whose structure adopts a common  $(\beta/\alpha)_8$  barrel conformation on the catalytic domain. Based on the alignment of two enzymes, the catalytic residue E186 of EndoS2, which corresponds to the general acid/base D235 of EndoS, is located on the fourth  $\beta$ -sheet. In order to explore the catalytic efficiency of transglycosylation of EndoS2, we set out to test whether conversion of amino acids near catalytic site would modulate the trasglycosylation activity. A few residues in the proximity of catalytic domain were chosen and mutated by site-directed mutagenesis by following general method 1, which contained T138 on the third  $\beta$ -sheet, D182 on the fourth  $\beta$ -sheet, and D226, T227 and T228 on the fifth  $\beta$ -sheet (Figure 1a, 1b).

```
1  MDKHLLVKRTLGCVCAATLMGAALATHHDSLNTVKAEEKTVQTKTDQQVQAKLVQEIIEGKRGPLYAGYFRTWHDRAST 80
81  GIDGKQQHPENTMAEVPKEVDILFVFDHTASDSPFWSELKDSYVHKLHQQTALVQ138IGVNELNGRTGLSKDYPTPEG 160
161  NKALAAAIVKAFVTD182RGVDGLD182IDIEHEFTNKRTPEEDARALNVFKEIAQLIGKNGSDKSKLLIM226,227,228D226T227LSVENNPIFKGI 240
241  AEDLDYLLRQYYGSQGGAEVDTINSDWNQYQNYIDASQFMIGSFFFEESASKGNLWFDVNEYDPNNPEKGDIEGTRAK 320
321  KYAEWQPSTGGLKAGIFS182Y182AIDRDGV182AHVPSTYKNRTSTNLQRHEVDNISHTDYTVSRK182LKTLMTEDKRYDVIDQKDIPD 400
401  PALREQIIQQVGGYKGD182LERYNKTLVLTGDKI182QNLKGLEKLSKLQKLELRQLSNVKEITPELLPESMKKDAELVMVGMTG 480
481  LEKLNLSGLNRQTL182DGIDVNSITHLTSFDISHNSLDLSEKSEDRKLLMTLMEQVSNHQKITVKN182TAFENQKPKGYYPQTY 560
561  DTKEGHYDVDAEHDILTDFVFGTVTKRNTFIGDEEAF182AIYKEGAVDGRQYVSKDYTYEAFRKYKGYKVHLTASNLGET 640
641  VTSKVTATTD182ETYLVDVSDGEKVVHMKLNIGSGAIMMENLAKGAKVIGTSGDFEQAKKIFDGEKSDRFFFTWGQTNWIAF 720
721  DLGEINLAKEWRLFNAETNTEIKTDS182SLNVAKGRLQILKDTTIDLEKMDIKNRKEYLSNDENWTDVAQMDDAKAIFNSKL 800
801  SNVLSRYWRFCDVGGASSYYPQYTELQILGQRLSNDVANTLKD 843
```

**Figure S1a:** The sequence of wild type EndoS2 and potential amino acid residues near the active site selected for site directed mutagenesis.

Endo S2	37	138	182	226	227	228	843
Endo S2	E	T	D	D	T	T	D
SEQ ID NO.1d (T138D)	_____	D	_____	_____	_____	_____	_____
SEQ ID NO.1e (T138E)	_____	E	_____	_____	_____	_____	_____
SEQ ID NO.1f (T138F)	_____	F	_____	_____	_____	_____	_____
SEQ ID NO.1h (T138H)	_____	H	_____	_____	_____	_____	_____
SEQ ID NO.1k (T138K)	_____	K	_____	_____	_____	_____	_____
SEQ ID NO.1l (T138L)	_____	L	_____	_____	_____	_____	_____
SEQ ID NO.1m (T138M)	_____	M	_____	_____	_____	_____	_____
SEQ ID NO.1n (T138N)	_____	N	_____	_____	_____	_____	_____
SEQ ID NO.1q (T138Q)	_____	Q	_____	_____	_____	_____	_____
SEQ ID NO.1r (T138R)	_____	R	_____	_____	_____	_____	_____
SEQ ID NO.1v (T138V)	_____	V	_____	_____	_____	_____	_____
SEQ ID NO.1w (T138W)	_____	W	_____	_____	_____	_____	_____
SEQ ID NO.2 (D182Q)	_____	_____	Q	_____	_____	_____	_____
SEQ ID NO.3 (D226Q)	_____	_____	_____	Q	_____	_____	_____
SEQ ID NO.4 (T227Q)	_____	_____	_____	_____	Q	_____	_____
SEQ ID NO.5 (T228Q)	_____	_____	_____	_____	_____	Q	_____

**Figure S1b:** Amino acid sequence of EndoS2 mutants.

As depicted in Fig. S1b, EndoS2 mutants T138D (SEQ ID NO.1d), T138E (SEQ ID NO.1e), T138F (SEQ ID NO.1f), T138H (SEQ ID NO.1h), T138K (SEQ ID NO.1k), T138L (SEQ ID NO.1l), T138M (SEQ ID NO.1m), T138N (SEQ ID NO.1n), T138Q (SEQ ID NO.1q), T138R (SEQ ID NO.1r), T138V (SEQ ID NO.1v), T138W (SEQ ID NO.1w), D182Q (SEQ ID NO. 2), D226Q (SEQ ID NO. 3), T227Q (SEQ ID NO. 4), and T228Q (SEQ ID NO. 5) were expressed in *E. coli* in high yield as His-tag fusion proteins and purified by the Ni-NTA affinity column.

#### 4 The glycan hydrolytic activity of EndoS2 mutants

The glycan hydrolytic activity of EndoS2 mutants was measured by using following general procedure.

**Procedure:** A solution containing 52  $\mu$ M commercial rituximab (400  $\mu$ g) and 52 nM EndoS2 or its selected mutant proteins in 100 mM HEPES buffer pH 7.0 was incubated at 37  $^{\circ}$ C with 700 rpm shaking. At the indicated time points, 2  $\mu$ g aliquots were taken and analyzed by 10% SDS-PAGE. Rituximab with glycan hydrolyzed would display faster migration on PAGE. The relative percentage of hydrolyzed

product was calculated by using Image J software based on the intensity of bands on SDS-PAGE (Fig. 2B).

.....

## 5 Chemo-enzymatic synthesis of N-linked glycans

**Materials and Methods.** All reagents were purchased from Sigma Aldrich, Across and used without further purification. Dry solvents were purchased from a commercial source without further distillation. Pulverized Molecular Sieves MS-4Å (Aldrich) for glycosylation was activated by heating at 350°C for 3 h. Reactions were monitored by analytical thin-layer chromatography (TLC) in EM silica gel 60 F254 plates and visualized under UV (254 nm) and/or by staining with acidic ceric ammonium molybdate or *p*-anisadehyde. Flash chromatography was performed on silica gel (Merck) of 40-63 µm particle size. All <sup>1</sup>H NMR and <sup>13</sup>C NMR spectra were recorded on a Bruker AVANCE 400 (400 MHz) spectrometer at 25°C. All <sup>1</sup>H Chemical shifts (in ppm) were assigned according to CDCl<sub>3</sub> (δ = 7.24 ppm) and D<sub>2</sub>O (δ = 4.80 ppm). Coupling constants (*J*) are reported in hertz (Hz). High resolution ESI mass spectra were recorded on a Bruker Daltonics spectrometer.

### ***Method A : Glycosylation by Fluoride-glycan Donor***

A mixture of silver triflate (5 eq.), bis (cyclopentadienyl) hafnium dichloride (3.5 eq.) and 4Å activated molecular sieves in dry toluene was stirred at room temperature for 1 h. The reaction mixture was then cooled to -50°C, a solution of *acceptor* (1.0 eq.) and donor (1.2~1.5 eq.) in toluene was added. The mixture was stirred at -10°C for 2-8 h. After TLC indicated complete consumption of acceptor, the reaction was quenched with Et<sub>3</sub>N, diluted with EtOAc and filtered through Celite. The filtrate was washed with aqueous NaHCO<sub>3</sub>, and a brine solution. The organic layers was dried over Na<sub>2</sub>SO<sub>4</sub> and concentrated in *vacuo*. The crude was purified by silica gel column

chromatography (toluene/ethyl acetate as elution system) to give product (the yield is shown on the scheme).

***Method B : Deprotection of Benzylidene***

*p*-Toluenesulfonic acid (*p*TSA, 1.5 eq.) was added to solution of starting material (1.0 eq.) in ACN/MeOH (2/1). Reaction was stirred at room temperature and monitored by thin-layer chromatography (TLC) analysis. After the benzylidene group was removed completely, the reaction was quenched by triethylamine and then concentrated. The crude was purified by silica gel column chromatography (toluene/ethyl acetate as elution system) to give the desired product.

***Method C : Glycosylation by thio-glycoside Donor***

A mixture of acceptor (1 eq.), thiomannoside donor (1.2-1.5 eq.) and activated 4 Å molecular sieves in CH<sub>3</sub>CN (10 mL) was stirred at room temperature for 1 h. The resulting mixture was cooled to -10°C, tris(4-bromophenyl)aminium hexachloroantimonate (1.5-2 eq.) was added and stirred at room temperature. TLC (ethyl acetate : toluene) indicated formation of product with consumption of starting material, reaction was quenched by Et<sub>3</sub>N. The reaction mixture was diluted with CH<sub>2</sub>Cl<sub>2</sub> and filtered through Celite. The filtrate was washed with aqueous NaHCO<sub>3</sub> (2 x 50 mL), and a brine (50 mL) solution. The organic layers was dried over Na<sub>2</sub>SO<sub>4</sub> and concentrated in *vacuo*. The crude was purified by silica gel column chromatography (toluene/ethyl acetate as elution system) to give product (the yield is shown on the scheme).

***Method D: Global Deprotection***

A mixture of protected oligosaccharides (50 mmol) and 10 mL of ethylene diamine: *n*BuOH (1/4) were stirred at 90°C overnight. Volatiles were evaporated, and crude

was reacted with 10 mL Ac<sub>2</sub>O/pyridine (1/2) overnight. The solvents were removed using high vacuum, and the product was purified by flash column chromatography (acetone/toluene as elute system). The products were de-acetylated using sodium methoxide in MeOH (10 mL) overnight. Reactions were neutralized by using IR-120, then, filtered and concentrated in vacuum. The residues were purified by flash column chromatography (acetone/toluene as elute system). The products were dissolved in 10 mL MeOH : H<sub>2</sub>O : HCOOH (6/3/1), Pd(OH)<sub>2</sub> (50% by weight) was added, and the reactions were hydrogenated overnight. The reaction mixtures were filtered through celite and concentrated in *vacuo*. The residues were purified by P2-Biogel column chromatography using water as eluent. The products were lyophilized to get white color powders (the yield is shown on the scheme).

***Method E : Enzymatic  $\alpha$  (2,6) Sialylation***

Glycans (5  $\mu$ mol), Neu5Ac (10  $\mu$ mol), ATP (0.05  $\mu$ mol), CTP (1  $\mu$ mol), phosphoenolpyruvate (10  $\mu$ mol, monopotassium salt), cytidine monophosphate kinase (CMK, 80 units), CMP-sialic acid synthetases (CSS, 120 units), pyruvate kinase (PK, 40 units), pyrophosphatase (PPA, 40 units) and  $\alpha$  2,6 sialyltransferase (150 units) were dissolved in 50  $\mu$ mol Tris buffer (25 mM, pH 7.5). The reaction was incubated at 37 °C with gentle agitation. Complete consumption of starting material was confirmed by mass spectrometric analysis. The reaction mixture was centrifuged and the supernatant subjected to gel filtration over P2-Biogel (eluent water). Fractions containing the product were combined and lyophilized to give the respective products as amorphous white solids.

## Glycan synthesis

Diverse set of N-glycan including high mannose, hybrid, and complex types were selected to test the transglycosylation activity of EndoS2 mutants at Rituximab Fc region. (Fig. S2).

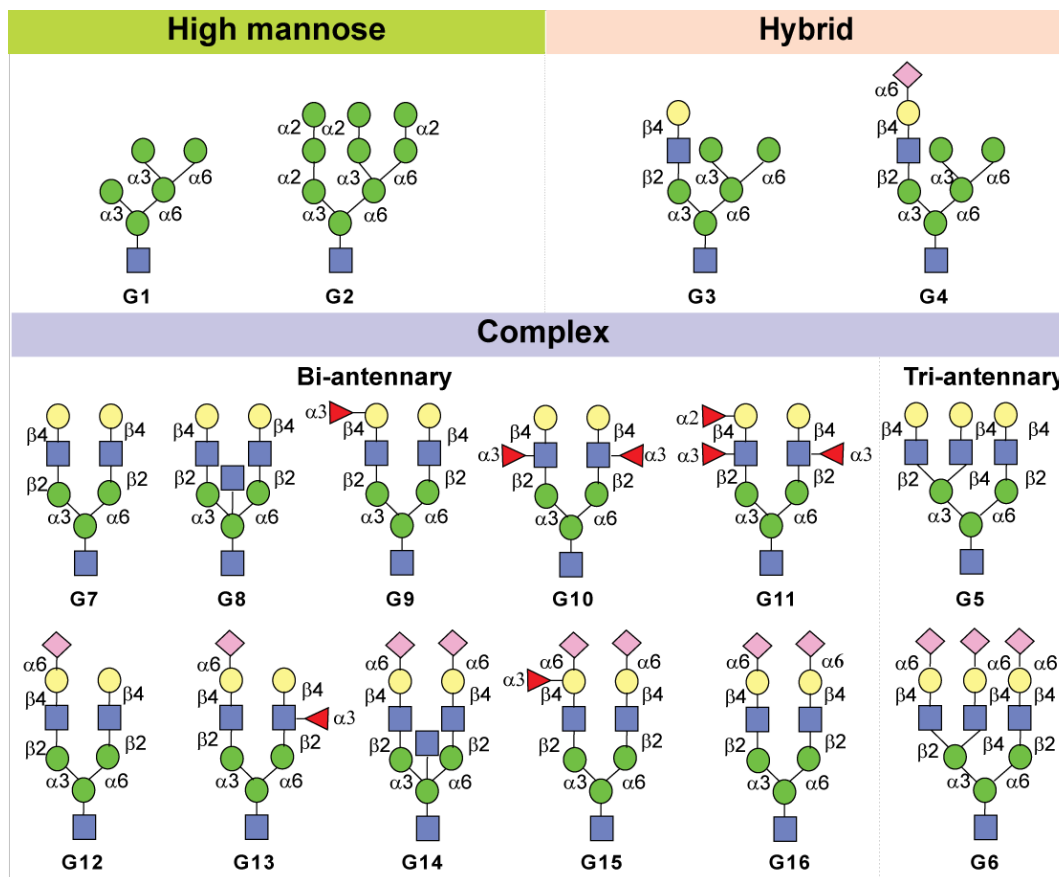


**Figure S2 :** Structures of N-linked glycans selected for homogeneous glycosylation of Rituximab.

Bi-antennary complex type glycans G7, G8, G14, and G16 were obtained according to our previous report <sup>[1]</sup> whereas; chemoenzymatic synthesis of glycans G9-G11, G13, and G15 will be reported elsewhere (unpublished results). Synthesis of glycans G1-G6 was commenced with gram scale production of all the necessary building blocks as shown in Figure S3. The stereo- and regioselective glycosylations of modular set of building blocks under the catalysis of appropriate promoters was performed to get series of high mannose, hybrid, bi- and tri-antennary complex

glycans (Scheme S1-S3). The structures obtained were characterized by  $^1\text{H}$ NMR and mass spectrometry (Table S1).

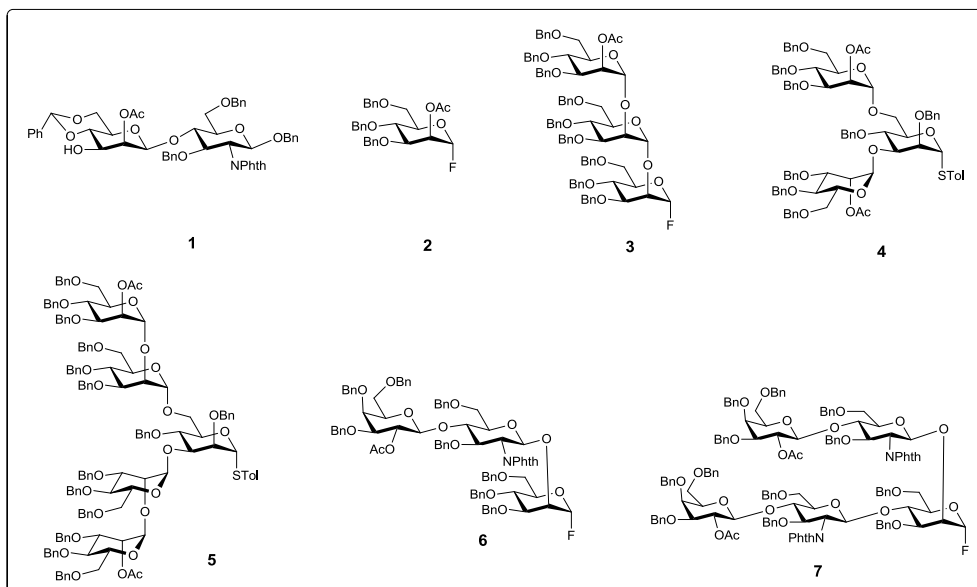
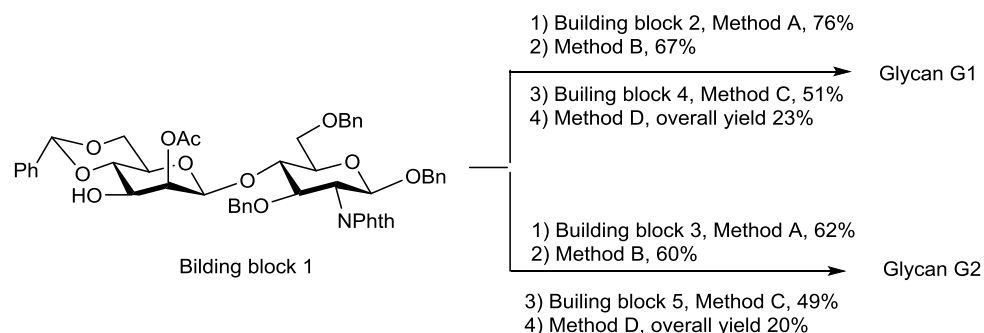
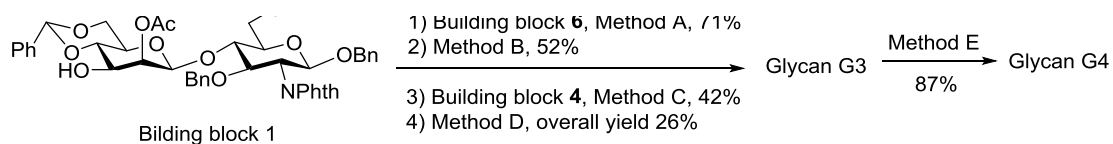


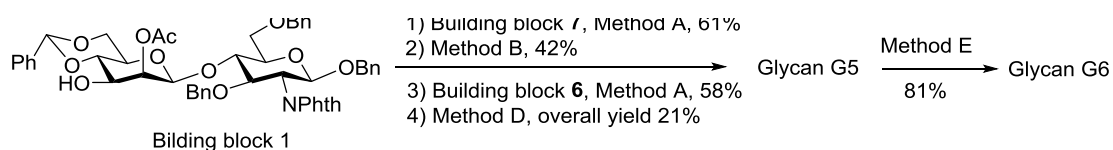
**Figure S3** : Modular set of building blocks used in glycan assembly.



**Scheme S1**: Preparation of high mannose type N-glycans G1/G2.

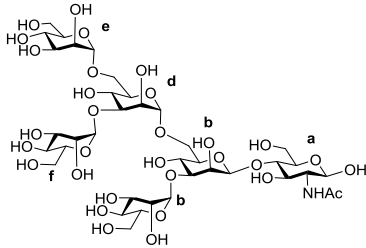
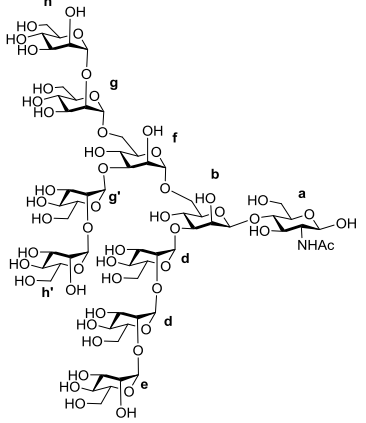
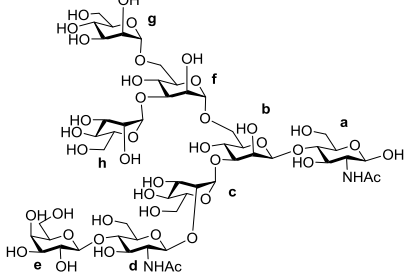


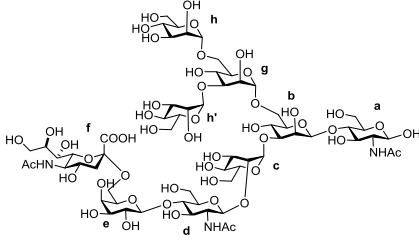
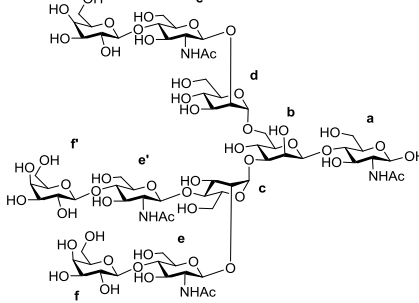
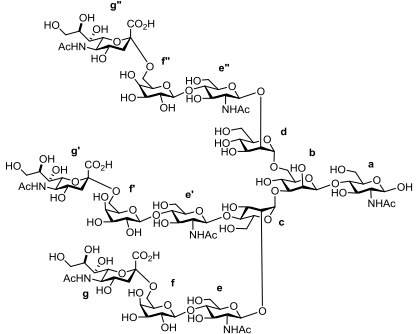
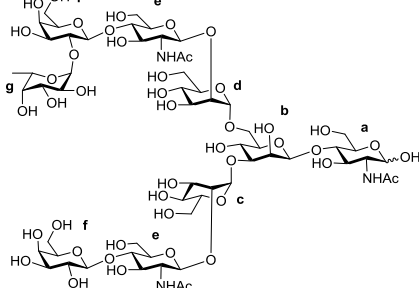
**Scheme S2**: Preparation of hybrid type N-glycans G3/G4.



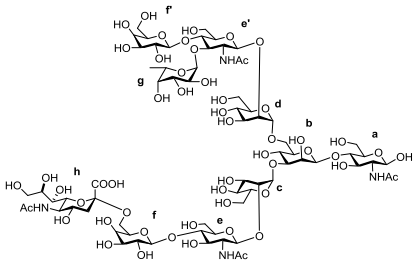
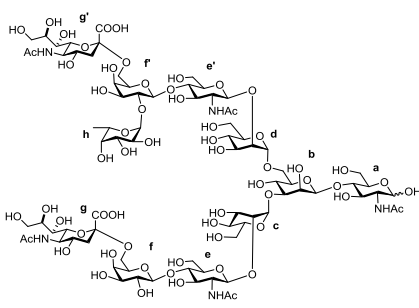
**Scheme S3**: Preparation of tri-antennary complex type N-glycans G5/6.

**Table S1: Characterization data of N-glycans**

Code	Chemical structure	<sup>1</sup> HNMR (400 MHz D <sub>2</sub> O) and Mass
G1		<sup>1</sup> HNMR (400 MHz, D <sub>2</sub> O): δ 5.27 (d, <i>J</i> = 3.6 Hz, 1H), 5.15 (s, 2H), 5.10 (d, <i>J</i> = 1.2 Hz, 1H), 4.93 (s, 1H), 4.90 (s, 1H), 4.29 (d, <i>J</i> = 3.6 Hz, 1H), 4.17-4.16 (m, 2H), 4.11-4.08 (m, 2H), 4.00-3.61 (m, 28H), 2.10 (s, 3H). ESI-MS: <i>m/z</i> calcd for C <sub>38</sub> H <sub>65</sub> NO <sub>31</sub> ; 1031.9156 found 1054.3403 ( <i>M</i> +Na) <sup>+</sup> .
G2		<sup>1</sup> HNMR (400 MHz, D <sub>2</sub> O): δ 5.42 (s, H), 5.36 (s, 1H), 5.33 (s, 1H), 5.26 (d, <i>J</i> = 4.4 Hz, 1H), 5.17 (s, 1H), 5.08-5.00 (m, 3H), 4.89 (s, 1H), 4.27-4.25 (m, 1H), 4.18 (s, 1H), 4.09-4.08 (m, 6H), 4.00-3.60 (m, 50H), 2.10 (s, 3H). ESI-MS: <i>m/z</i> calcd for C <sub>62</sub> H <sub>105</sub> NO <sub>51</sub> ; 1679.4853 found 1702.5501 ( <i>M</i> +Na) <sup>+</sup> .
G3		<sup>1</sup> HNMR (400 MHz, D <sub>2</sub> O): δ 5.22 (d, <i>J</i> = 3.6 Hz, 1H), 5.10 (s, 1H), 4.89 (s, 1H), 4.85 (d, <i>J</i> = 1.2 Hz, 1H), 4.77 (s, 1H), 4.55 (d, <i>J</i> = 8.0 Hz, 1H), 4.45 (d, <i>J</i> = 8.0 Hz, 1H), 4.23 (s, 1H), 4.19 (d, <i>J</i> = 3.1 Hz, 1H), 4.13 (d, <i>J</i> = 3.1 Hz, 1H), 4.05-3.45 (m, 40H), 2.03 (s, 3H), 2.02 (s, 3H). ESI-MS: <i>m/z</i> calcd for C <sub>52</sub> H <sub>88</sub> N <sub>2</sub> O <sub>41</sub> ; 1396.4863 found 1419.4746 ( <i>M</i> +Na) <sup>+</sup> .

G4	 <p>Chemical structure of a branched oligosaccharide with labels a-h and h'.</p>	<sup>1</sup> HNMR (400 MHz, D <sub>2</sub> O): δ 5.23 (d, <i>J</i> = 3.6 Hz, 1H), 5.12 (s, 1H), 5.06 (s, 1H), 4.90 (s, 1H), 4.87 (s, 1H), 4.60 (d, <i>J</i> = 8.1 Hz, 1H), 4.43 (d, <i>J</i> = 8.0 Hz, 1H), 4.26 (s, 1H), 4.20 (d, <i>J</i> = 2.1 Hz, 1H), 4.13 (d, <i>J</i> = 2.8 Hz, 1H), 4.00-3.50 (m, 53H), 2.64 (dd, <i>J</i> = 4.8 and 12.1 Hz, 1H), 2.06 (s, 3H), 2.03 (s, 3H), 2.02 (s, 3H), 1.72 (t, <i>J</i> = 12.2 Hz, 1H). ESI-MS: <i>m/z</i> calcd for C <sub>63</sub> H <sub>105</sub> N <sub>3</sub> O <sub>49</sub> ; 1687.5896 found 1686.5769 ( <i>M</i> - H) <sup>-</sup> .
G5	 <p>Chemical structure of a branched oligosaccharide with labels a-f and f'.</p>	<sup>1</sup> HNMR (400 MHz, D <sub>2</sub> O): δ 5.22 (d, <i>J</i> = 3.2 Hz, 1H), 5.13 (s, 1H), 4.94 (s, 1H), 4.60-4.55 (m, 4H), 4.83 (dd, <i>J</i> = 2.4 and 8 Hz, 4H), 4.23 (s, 2H), 4.13 (s, 1H), 4.01-3.50 (m, 56H), 2.09 (s, 3H), 2.07 (s, 3H), 2.06 (s, 6H). ESI-MS: <i>m/z</i> calcd for C <sub>68</sub> H <sub>114</sub> N <sub>4</sub> O <sub>51</sub> ; 1802.6425 found 1825.6313 ( <i>M</i> + Na) <sup>+</sup> and 924.3066 ( <i>M</i> + Na) <sup>2+</sup> .
G6	 <p>Chemical structure of a branched oligosaccharide with labels a-g and g'.</p>	<sup>1</sup> HNMR (400 MHz, D <sub>2</sub> O): δ 5.24 (d, <i>J</i> = 3.2 Hz, 1H), 5.15 (s, 1H), 4.93 (s, 1H), 4.64-4.62 (m, 4H), 4.90-4.45 (m, 4H), 4.29 (bs, 1H), 4.23-4.13 (m, 3H), 4.13 (bs, 1H), 4.01-3.59 (m, 76H), 2.68 (dd, <i>J</i> = 3.2 and 12.0, 3H), 2.10 (s, 9H), 2.09 (s, 6H), 2.01 (s, 6H), 1.77 (t, <i>J</i> = 12.2 Hz, 3H). ESI-MS: <i>m/z</i> calcd for C <sub>101</sub> H <sub>165</sub> N <sub>7</sub> O <sub>75</sub> ; 2677.9354 found 891.3063 ( <i>M</i> - H) <sup>3-</sup> .
G9	 <p>Chemical structure of a branched oligosaccharide with labels a-g and g'.</p>	<sup>1</sup> HNMR (400 MHz, D <sub>2</sub> O): δ 5.20 (d, <i>J</i> = 2.8 Hz, 1H), 5.11 (d, <i>J</i> = 2.8 Hz, 1H), 5.02 (s, 1H), 4.83 (s, 1H), 4.47 (d, <i>J</i> = 10 Hz, 2H), 4.37 (d, <i>J</i> = 8, 1H), 4.12-4.10 (m, 2H), 4.07 (s, 1H), 4.01 (d, <i>J</i> = 2 Hz, 1H), 3.89-3.34 (m, 50H), 1.95 (s, 6H), 1.87 (s,

		3H), 1.13 (d, $J = 6.8$ Hz, 3H). ESI-MS: $m/z$ calcd for $C_{60}H_{101}N_3O_{45}$ ; 1583.5745 found 814.7733 ( $M + Na$ ) <sup>2+</sup> .
G10		<sup>1</sup> HNMR (400 MHz, D <sub>2</sub> O): $\delta$ 5.20 (d, $J = 3.2$ Hz, 1H), 5.12 (t, $J = 3.67$ Hz, 2H), 5.10 (s, 1H), 4.90 (s, 1H), 4.58 (d, $J = 7.6$ Hz, 2H), 4.44 (d, $J = 7.6$ , 2H), 4.25 (bs, 1H), 4.18 (bs, 1H), 4.09 (bs, 1H), 3.97-3.60 (m, 49H), 3.57-3.48 (m, 4H), 2.05 (s, 3H), 2.05 (s, 3H), 2.03 (s, 3H), 1.17 (d, $J = 6.4$ Hz, 6H). ESI-MS: $m/z$ calcd for $C_{66}H_{111}N_3O_{49}$ ; 1729.6325 found 1753.6105 ( $M + Na$ ) <sup>+</sup> and 887.7995 ( $M + Na$ ) <sup>2+</sup> .
G11		<sup>1</sup> HNMR (400 MHz, D <sub>2</sub> O): $\delta$ 5.26 (d, $J = 3.2$ Hz, 1H), 5.20 (d, $J = 2.8$ Hz, 1H), 5.12 (t, $J = 4.0$ Hz, 2H), 5.10 (s, 1H), 4.97 (s, 1H), 4.49 (d, $J = 7.6$ , 1H), 4.45 (d, $J = 7.8$ Hz, 1H), 4.24 (bs, 2H), 4.18 (bs, 1H), 4.10 (bs, 1H), 3.97-3.44 (m, 59H), 2.05 (s, 3H), 2.05 (s, 3H), 2.03 (s, 3H), 1.26-1.21 (m, 6H), 1.17 (d, $J = 6.4$ Hz, 3H). ESI-MS: $m/z$ calcd for $C_{83}H_{140}N_4O_{61}$ ; 1875.7356 found 960.8311 ( $M + Na$ ) <sup>2+</sup> .
G12		<sup>1</sup> HNMR (400 MHz, D <sub>2</sub> O): $\delta$ 5.19 (s, 1H), 5.12 (s, 1H), 4.91 (s, 1H), 4.50 (t, $J = 7.2$ Hz, 2H), 4.44 (t, $J = 8$ Hz, 2H), 4.25 (s, 1H), 4.18 (s, 1H), 4.0 (s, 1H), 3.97-3.50 (m, 55H), 2.66 (dd, 1H), 2.05 (s, 3H), 2.04 (s, 3H), 2.03 (s, 3H), 2.01 (s, 3H), 1.17 (t, $J = 10.2$ Hz, 1H). ESI-MS: $m/z$ calcd for $C_{65}H_{108}N_4O_{49}$ ; 1728.6125 found 1727.6131 ( $M - H$ ) <sup>-</sup> .

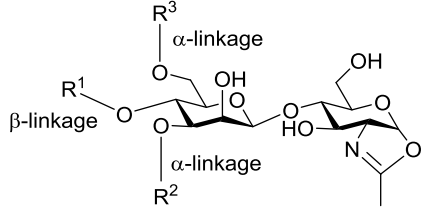
G13		$^1\text{H NMR}$ (400 MHz, $\text{D}_2\text{O}$ ): $\delta$ 5.13 (d, $J = 2.4$ Hz, 1H), 5.05 (s, 2H), 4.84 (s, 2H), 4.52 (t, $J = 4.0$ Hz, 3H), 4.37 (d, $J = 7.6$ Hz, 2H), 4.18 (s, 1H), 4.11 (s, 1H), 4.02 (s, 1H), 3.90-3.39 (m, 58H), 4.11 (s, 1H), 3.9 (s, 1H), 3.97-3.50 (m, 55H), 2.60 (d, $J = 2$ Hz, 1H), 1.98 (s, 3H), 1.96 (s, 3H), 1.95 (s, 6H), 1.61 (t, $J = 3.6$ Hz, 1H), 1.0 (d, $J = 6.44$ Hz, 3H). ESI-MS: $m/z$ calcd for $\text{C}_{71}\text{H}_{118}\text{N}_4\text{O}_{53}$ ; 1874.6745 found 1773.6544 ( $M - \text{H}$ ) $^-$ .
G15		$^1\text{H NMR}$ (400 MHz, $\text{D}_2\text{O}$ ): $\delta$ 5.33 (s, 1H), 5.22 (d, $J = 3.2$ Hz, 1H), 5.11 (s, 1H), 4.94 (s, 1H), 4.60-4.51 (m, 3H), 4.4 (d, $J = 8$ Hz, 1H), 4.25-4.11 (m, 4H), 3.98-3.48 (m, 67H), 2.70-2.61 (m, 2H), 2.07 (s, 3H), 2.06 (s, 3H), 2.05 (s, 3H), 2.04 (s, 3H), 2.02 (s, 3H), 1.74-1.60 (m, 2H), 1.22 (d, $J = 6.0$ Hz, 3H). ESI-MS: $m/z$ calcd for $\text{C}_{82}\text{H}_{135}\text{N}_5\text{O}_{61}$ ; 2163.7589 found 1081 ( $M - \text{H}$ ) $^{2-}$ .

\* Characterization data of glycans G7, G8, G14, and G16 is reported previously<sup>[1]</sup>

### Preparation of glycan-oxazolines

A solution of respective glycans G1-G16 (3-5 mg), 2-chloro-1, 3-dimethyl imidazolium chloride (DMC) (6-10 mg) and  $\text{Et}_3\text{N}$  (10-20  $\mu\text{L}$ ) in water (300-500  $\mu\text{L}$ ) was stirred at 4 $^\circ$  C. for 1 h. The reaction mixture was subjected to gel filtration chromatography on a Sephadex G-25 column eluted by 0.05% aqueous  $\text{Et}_3\text{N}$ . The fractions containing the products were combined and lyophilized to give a white powder (2.5-4 mg, Yield ~80-90%). The products were characterized by  $^1\text{H}$  NMR (Table S2).

**Table S2:** Characterization data of glycan oxazolines

 Glycan oxazoline general formula	
No.	<sup>1</sup> HNMR (400 MHz D <sub>2</sub> O)
G1	<sup>1</sup> HNMR (400 MHz, D <sub>2</sub> O): δ 5.95 (d, <i>J</i> = 7.2 Hz, 1H), 5.11 (d, <i>J</i> = 3.6 Hz, 2H), 4.95 (s, 3H), 4.78-4.72 (m, 3H), 4.65 (s, 2H), 4.13-4.08 (m, 6H), 3.86-3.08 (m, 28H), 1.77 (s, 3H).
G2	<sup>1</sup> HNMR (400 MHz, D <sub>2</sub> O): δ 6.00 (d, <i>J</i> = 7.2 Hz, 1H), 5.30 (s, 1H), 5.25 (s, 1H), 5.22 (s, 1H), 5.05 (s, 1H), 4.96-4.95 (m, 3H), 4.82 (s, 1H), 4.61 (s, 1H), 4.28-4.27 (s, 1H), 4.09-3.53 (m, 59H), 1.97 (s, 3H).
G4	<sup>1</sup> HNMR (400 MHz, D <sub>2</sub> O): δ 6.06 (d, <i>J</i> = 7.2 Hz, 1H), 5.12 (t, <i>J</i> = 4 Hz, 1H), 4.95 (bs, 3H), 4.73 (s, 1H), 4.58 (d, <i>J</i> = 7.2 Hz, 1H), 4.43 (d, <i>J</i> = 8 Hz, 1H), 4.34 (t, <i>J</i> = 2 Hz, 1H), 4.19-4.14 (m, 4H), 4.05-3.49 (m, 49H), 2.64 (dd, <i>J</i> = 4.8 & 12 Hz, 1H), 2.05 (s, 6H), 2.12 (s, 3H), 1.70 (t, <i>J</i> = 12.4 Hz, 1H).
G5	<sup>1</sup> HNMR (400 MHz, D <sub>2</sub> O): δ 6.07 (d, <i>J</i> = 6.8 Hz, 1H), 5.12 (s, 2H), 4.90 (s, 2H), 4.62-4.55 (m, 4H), 4.47-4.44 (m, 4H), 4.34 (s, 1H), 4.18-4.14 (m, 7H), 4.39-3.35 (m, 49H), 2.05 (s, 9H), 2.03 (s, 3H).
G6	<sup>1</sup> HNMR (400 MHz, D <sub>2</sub> O): δ 6.12 (d, <i>J</i> = 7.2 Hz, 1H), 5.14 (s, 1H), 4.65-4.62 (m, 2H), 4.49-4.45 (bs, 3H), 4.39 (s, 1H), 4.22 (bs, 6H), 3.99-3.56 (m, 75H), 2.70 (d, <i>J</i> = 4.8 & 12 Hz, 3H), 2.10 (s, 6H), 2.09 (s, 9H), 2.05 (s, 6H), 1.74 (t, <i>J</i> = 12 Hz, 3H).
G9	<sup>1</sup> HNMR (400 MHz, D <sub>2</sub> O): δ 6.06 (d, <i>J</i> = 7.2 Hz, 1H), 5.29 (d, <i>J</i> = 2.8 Hz, 1H), 5.13 (s, 1H), 4.96 (s, 1H), 4.56-4.51 (m, 3H), 4.47-4.40 (d, <i>J</i> = 8.2 Hz, 1H), 4.39 (s, 1H), 4.36-4.14 (m, 3H), 3.92-3.51 (m, 47H), 2.06 (s, 3H), 2.05 (s, 3H), 2.04 (s, 3H), 1.11 (d, <i>J</i> = 6.8 Hz, 3H).
G13	<sup>1</sup> HNMR (400 MHz, D <sub>2</sub> O): 6.09 (d, <i>J</i> = 7.1 Hz, 1H), 5.16 (s, 1H), 4.96 (s, 2H), 4.65 (t, <i>J</i> = 7.2 Hz, 2H), 4.61 (t, <i>J</i> = 7.2 Hz, 2H), 4.40 (s, 1H), 4.21-4.17 (m, 5H), 3.98-3.55 (m, 52H), 2.72 (d, <i>J</i> = 11.6 Hz, 1H), 2.09 (s, 6H), 2.08 (s, 3H), 2.05 (s, 3H), 1.75 (t, <i>J</i> = 10.6 Hz, 1H), 1.20 (d, <i>J</i> = 6.6

Hz, 3H).

\* Characterization data of oxazolines of glycans G7, G8, G14, and G16 is reported previously<sup>[1]</sup>.

## 6 The transglycosylation potential of EndoS2 and its mutants to core fucosylated/afucosylated Rituximab

The transglycosylation ability of EndoS2 and its mutants was then examined using the Rtx-N and Rtx-NF as the acceptor and alpha 2, 6 sialylated bi-antennary complex type, (SCT, glycan G16) oxazoline as the donor substrates.

**Procedure :** A solution containing 67.5  $\mu$ M Rtx-N/Rtx-NF (400  $\mu$ g) and 2.5 mM SCT-oxazoline (200  $\mu$ g) in 100 mM HEPES buffer pH 7.0 was incubated with 67.5 nM EndoS2 or selected mutant proteins at 37 °C with 700 rpm shaking. At the indicated time points, 2  $\mu$ g aliquots were taken and analyzed by 10% SDS-PAGE. Glycosylated Rituximab would display slower migration on PAGE. The relative percentage of Rituximab-SCT was calculated by using Image J software based on the intensity of bands on SDS-PAGE (Fig. 3 and S4).

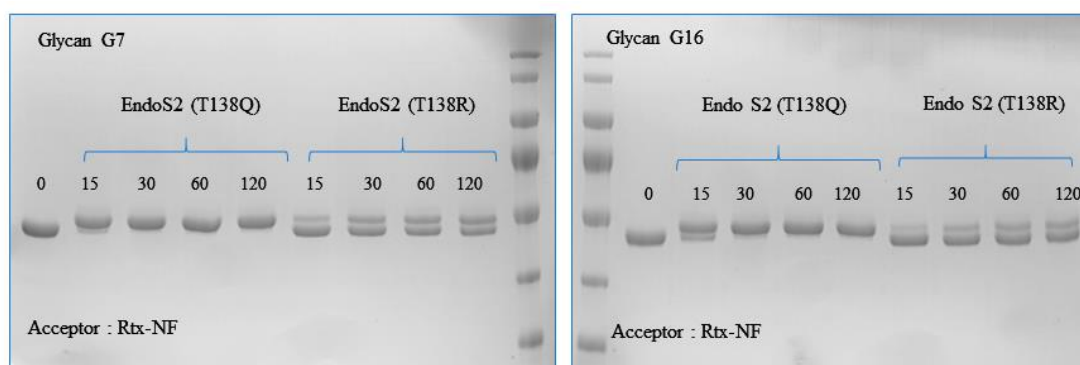


**Figure S4:** Transglycosylation activity of selected mutants of EndoS2 against bi-antennary glycans G7, and G16 using core fucosylated Rituximab (Rtx-NF) as an acceptor and glycan-oxazolines as donor substrates. The reaction progress was monitored by sodium dodecyl sulfate polyacrylamide gel electrophoresis (SDS-PAGE).

## 7 Transglycosylation of GlcNAc-Rituximab with various glycan oxazoline using EndoS2 mutants.

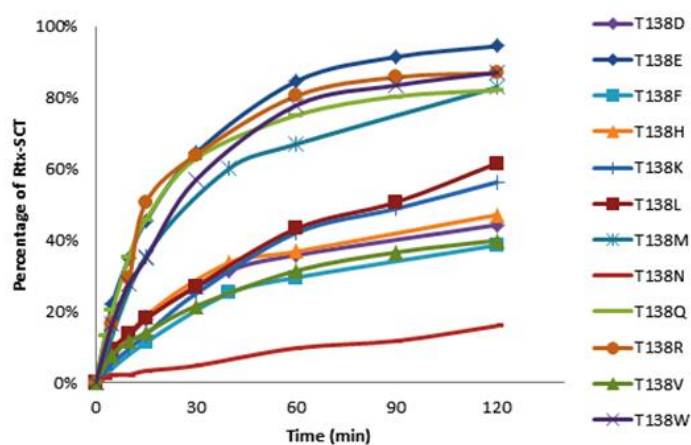


**Figure S5:** Comparison of the transglycosylation activity of variants with mutation at T138 using Rtx-N as an acceptor and  $\alpha$ -2, 6 sialylated bi-antennary complex type glycan (SCT)-oxazoline as a donor. The reaction mixture containing a T138 mutant (67.5 nM), Rtx-N (67.5  $\mu$ M), and SCT-oxazoline (2.5 mM) was incubated for 2 h and analyzed by SDS-PAGE. The relative percentages of Rituximab with  $\alpha$ -2, 6 sialylated bi-antennary complex type glycan at the Fc region (Rtx-SCT) is shown

To identify the optimal amino acid residue at the T138 site that would exhibit potent transglycosylation activity but devoid of hydrolytic activity, the transglycosylation activity of various mutations at this site (T138D, T138E, T138F, T138H, T138K, T138L, T138M, T138N, T138Q, T138R, T138V, and T138W) were examined using Rtx-N as acceptor and SCT-oxazoline as donor. The results indicated that most of the mutants at T138 showed better glycosynthase activity; however, the mutants such as T138E, T138M, T138Q, T138R, and T138W showed excellent transglycosylation potency (Fig. S5). The mutant T138N retained its hydrolytic activity, and the rest were moderate in their transglycosylation tendency

Transglycosylation of high mannose and hybrid glycans

To a mixture of Rtx-N (2 mg, 0.337 mM) in 100 mM HEPES buffer (pH 7.0) and respective glycan oxazolines G1-G4 (weight ratio of 1:1 for G1, G3, G4 and 1:1.5 for G2) was added selected mutants of EndoS2 including T138Q, D182Q, D226Q, T227Q, and T228Q (Rtx/enzyme weight ratio of 1/20 or 1/10) and incubated at 37 °C with 700 rpm shaking. At the indicated time points, 2 µg aliquots were taken and analyzed by 10% SDS-PAGE. Glycosylated Rituximab would display slower migration on PAGE. The relative percentage of Rituximab-SCT was calculated by using Image J software based on the intensity of bands on SDS-PAGE and best results are shown in Fig. S6.

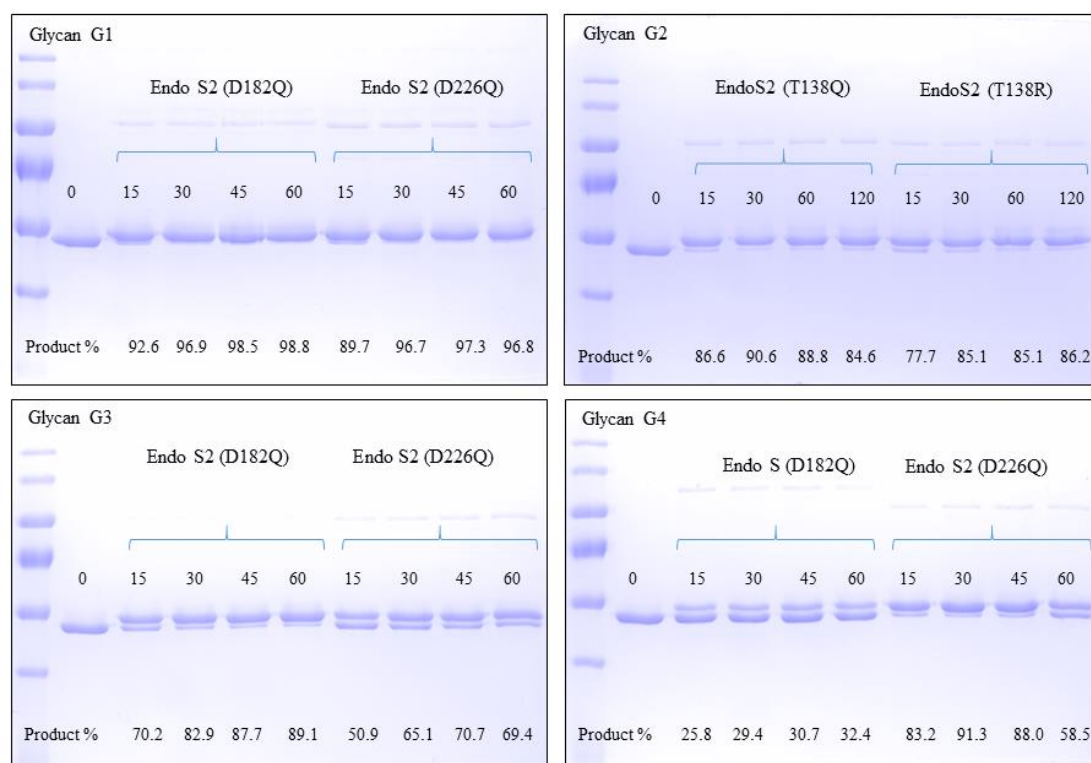


**Figure S6:** Transglycosylation activity of selected mutants of EndoS2 against high mannose type  $\text{Man}_5\text{GlcNAc}_2$  (glycan G1),  $\text{Man}_9\text{GlcNAc}_2$  (glycan G2) and hybrid series glycans (G3 and G4), using GlcNAc-Rituximab as an acceptor and glycan-oxazolines (G1-G4) as donor substrates. The reaction progress was monitored by sodium dodecyl sulfate polyacrylamide gel electrophoresis (SDS-PAGE). Lane 1:

marker; Lane 2: GlcNAc-Rituximab; time points are in Min.; product % is shown at the bottom.

#### Transglycosylation of tri-antennary complex type glycans

To a mixture of Rtx-N (2 mg, 0.337 mM) in 100 mM HEPES buffer (pH 7.0) and respective glycan oxazolines G4-G6 (weight ratio of 1:5) was added selected mutants of EndoS2 including T138Q, D182Q, D226Q, T227Q, and T228Q (Rtx/enzyme weight ratio of 1/20 or 1/10) and incubated at 37 °C with 700 rpm shaking. At the indicated time points, 2 µg aliquots were taken and analyzed by 10% SDS-PAGE. Glycosylated Rituximab would display slower migration on PAGE. The relative percentage of Rituximab-SCT was calculated by using Image J software based on the intensity of bands on SDS-PAGE and best results are shown in Fig. S7.

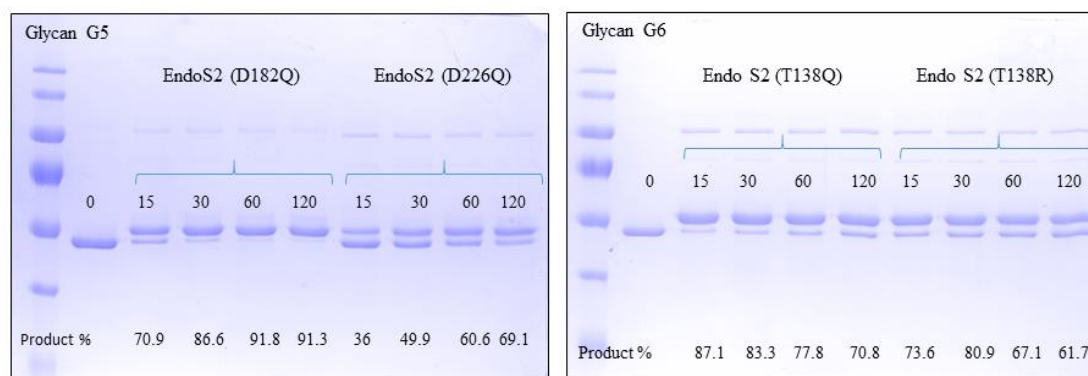


**Figure S7:** Transglycosylation activity of selected mutants of EndoS2 against tri-antennary complex type glycans (G5-6). The reaction was performed using Rtx-GlcNAc as an acceptor and glycan-oxazolines (G4-G5) as donor substrate. The reaction progress was monitored by sodium dodecyl sulfate polyacrylamide gel electrophoresis (SDS-PAGE). Lane 1: marker; Lane 2: Rtx-GlcNAc; time points are in min.; product % is shown at the bottom.

#### Transglycosylation of bi-antennary complex type glycans

To a mixture of Rtx-N (2 mg, 0.337 mM) in 100 mM HEPES buffer (pH 7.0) and selected glycan oxazolines G7-G10 (weight ratio of 1:1) was added selected mutants of EndoS2 including T138Q, D182Q, D226Q, T227Q, and T228Q (Rtx/enzyme weight ratio of 1/20) and incubated at 37 °C with 700 rpm shaking. At the indicated time points, 2 µg aliquots were taken and analyzed by 10% SDS-PAGE. The relative percentage of Rituximab-SCT was calculated by using Image J software based on the intensity of bands on SDS-PAGE and best results are shown in Fig. S8.

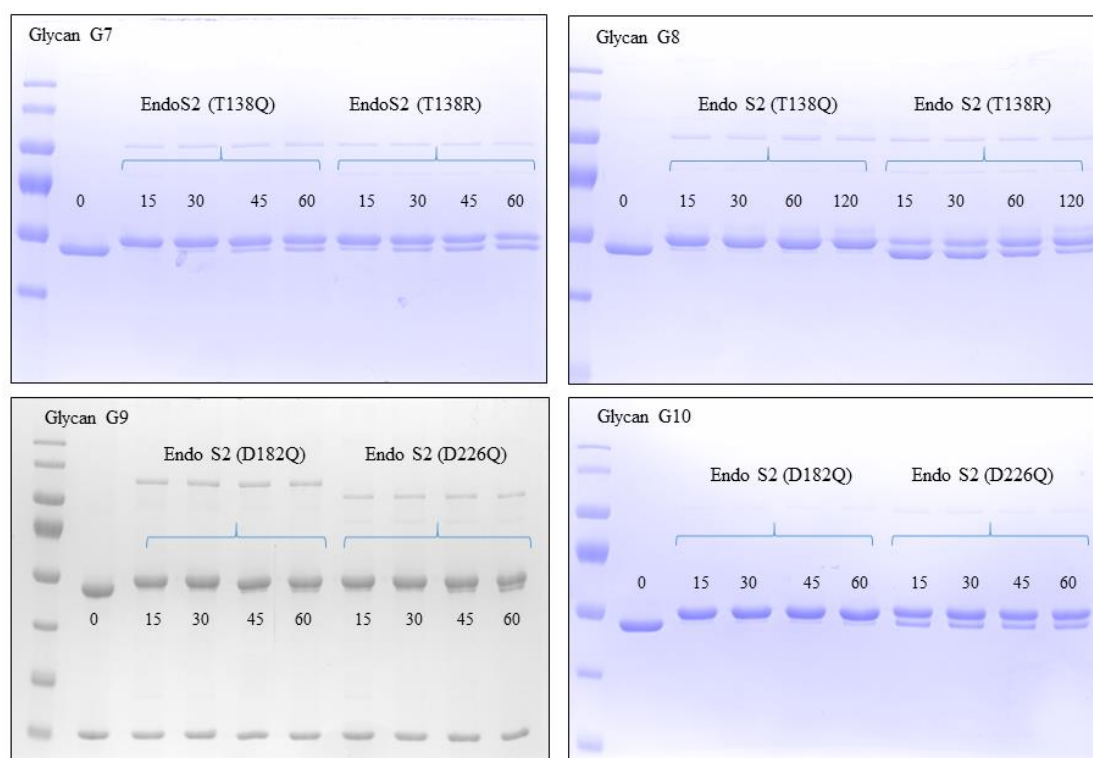


**Figure S8:** Transglycosylation activity of selected mutants of EndoS2 against series of bi-antennary complex type structures. The transglycosylation was performed using Rtx-GlcNAc as an acceptor and glycan-oxazolines (G7-G10) as donor substrate. The reaction progress was monitored by sodium dodecyl sulfate polyacrylamide gel electrophoresis (SDS-PAGE). Lane 1: marker; Lane 2: GlcNAc-Rituximab; time points are in Min.

## 8 Preparation of diverse Rituximab variants

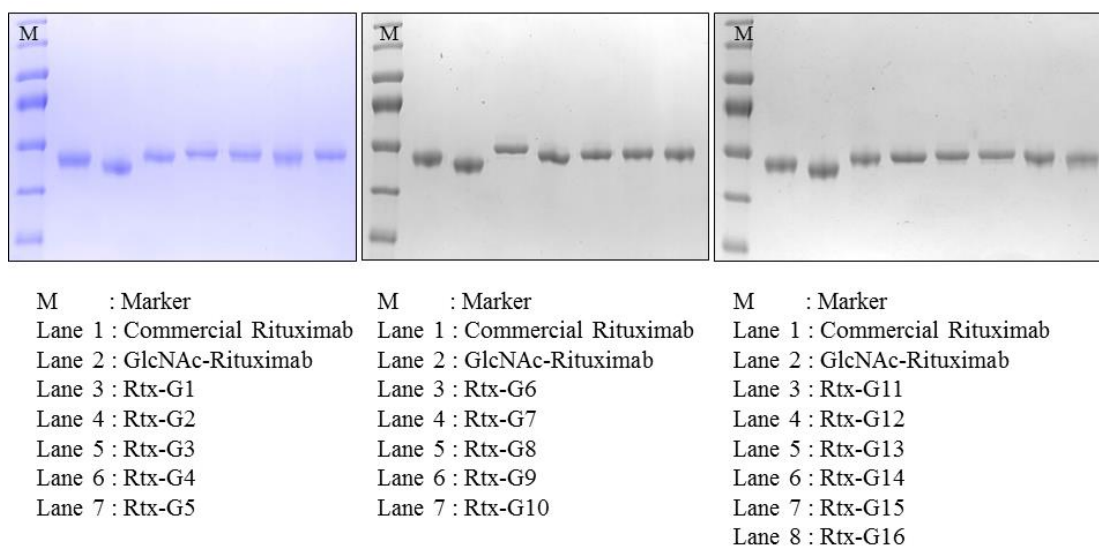
General procedure. To a mixture of Rtx-GlcNAc (2 mg, 0.337 mM) in 100 mM HEPES buffer (pH 7.0) and respective glycan oxazolines G1-G16 (2-3 mg) was added the desired EndoS2 mutant and incubated at 37 °C with 700 rpm shaking. The reaction was quenched by adding 0.1 mM of EDTA solution. The optimized reaction conditions including time, temperature, ratios of antibody/glycan oxazolines, and antibody/enzymes have been listed in Table S2.

Table S3 lists the optimized reaction details for preparation of each of the Rituximab glycoforms

Starting Material	Rituximab Glycoform	EndoS2 mutants	Enzyme	Glycan oxazoline	Glycan amount	Reaction time	Reaction Yield
Rtx-N (2 mg, 0.337 mM)	Rtx-G1	D226Q	16.8 $\mu$ M	G1	2 mg	30 min	72%
	Rtx-G2	T138Q	33.7 $\mu$ M	G2	3 mg	30 min	70%
	Rtx-G3	D182Q	16.8 $\mu$ M	G3	2 mg	30 min	75%
	Rtx-G4	D226Q	16.8 $\mu$ M	G4	2 mg	60 min	72%
	Rtx-G5	D182Q	16.8 $\mu$ M	G5	3 mg	30 min	70%
	Rtx-G6	D138Q	33.7 $\mu$ M	G6	3 mg	30 min	69%
	Rtx-G7	T138Q	16.8 $\mu$ M	G7	2 mg	30 min	89%
	Rtx-G8	T138Q	16.8 $\mu$ M	G8	2 mg	30 min	70%
	Rtx-G9	D182Q	16.8 $\mu$ M	G9	2 mg	30 min	65%
	Rtx-G10	D182Q	16.8 $\mu$ M	G10	2 mg	30 min	68%
	Rtx-G11	D182Q	16.8 $\mu$ M	G11	2 mg	60 min	71%
	Rtx-G12	D182Q	16.8 $\mu$ M	G12	2 mg	60 min	76%

	Rtx-G13	D138Q	16.8 $\mu$ M	G13	2 mg	30 min	68%
	Rtx-G14	D182Q	16.8 $\mu$ M	G14	3 mg	60 min	67%
	Rtx-G15	D182Q	16.8 $\mu$ M	G15	2 mg	60 min	58%
	Rtx-G16	D182Q	16.8 $\mu$ M	G15	2 mg	60 min	80%

The reaction mixtures were then purified with protein A affinity column, followed by anion exchange column capto Q on a fast protein liquid chromatography (FPLC) system to collect the desired products, anti-CD20 glycoengineered Rituximabs. The purity was confirmed by SDS-PAGE analysis (Figure S8). The products analyzed by intact mass to confirm the desired glycosylation pattern (Fig. S9-10).



**Figure S9:** SDS PAGE analysis of glycoengineered Rituximabs (Rtx G1-G16), Rtx-GlcNAc, and commercial Rituximab.

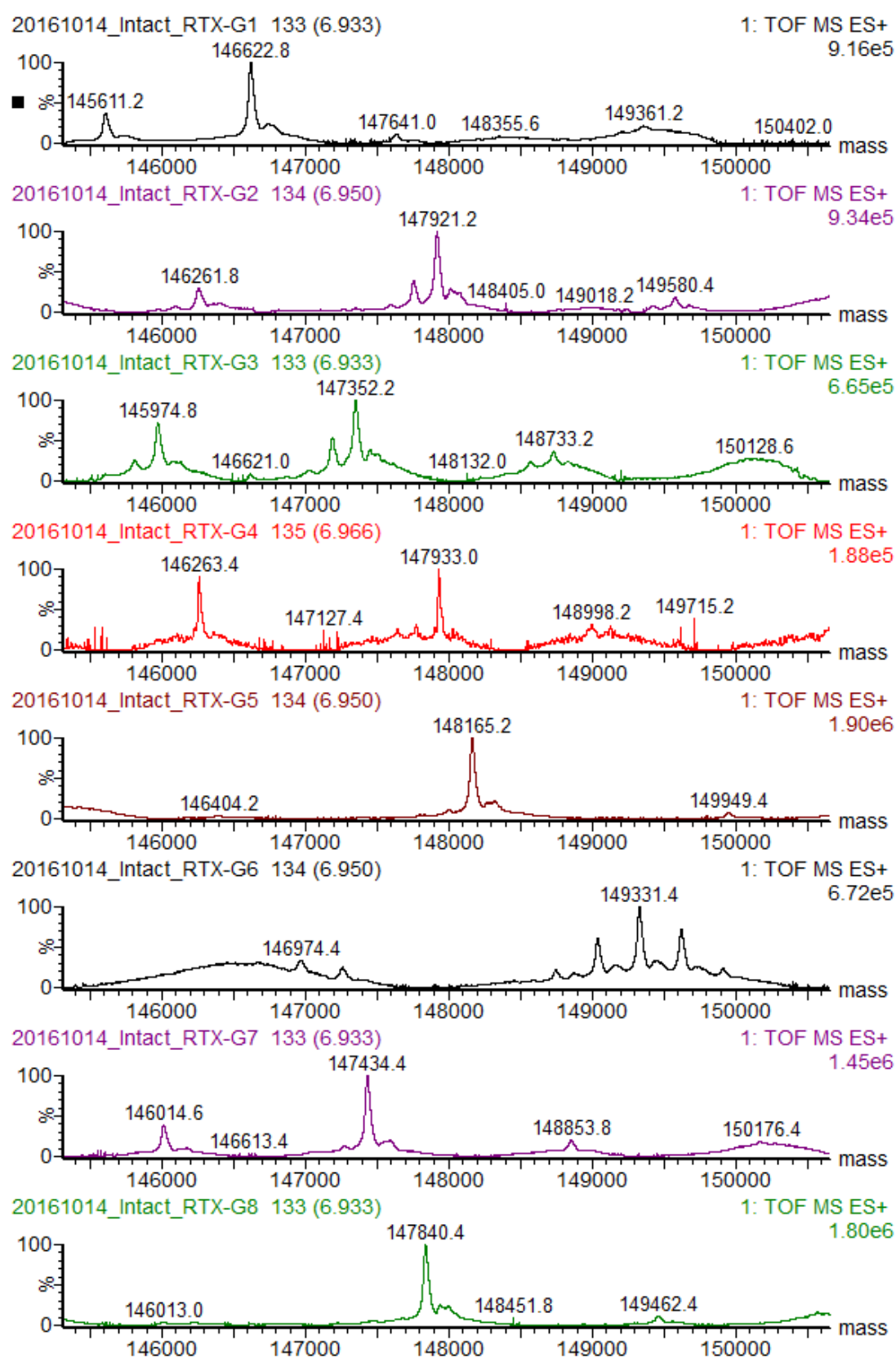


**Figure S10:** Intact mass analysis of glycoengineered antibodies (Rtx G1-G8)

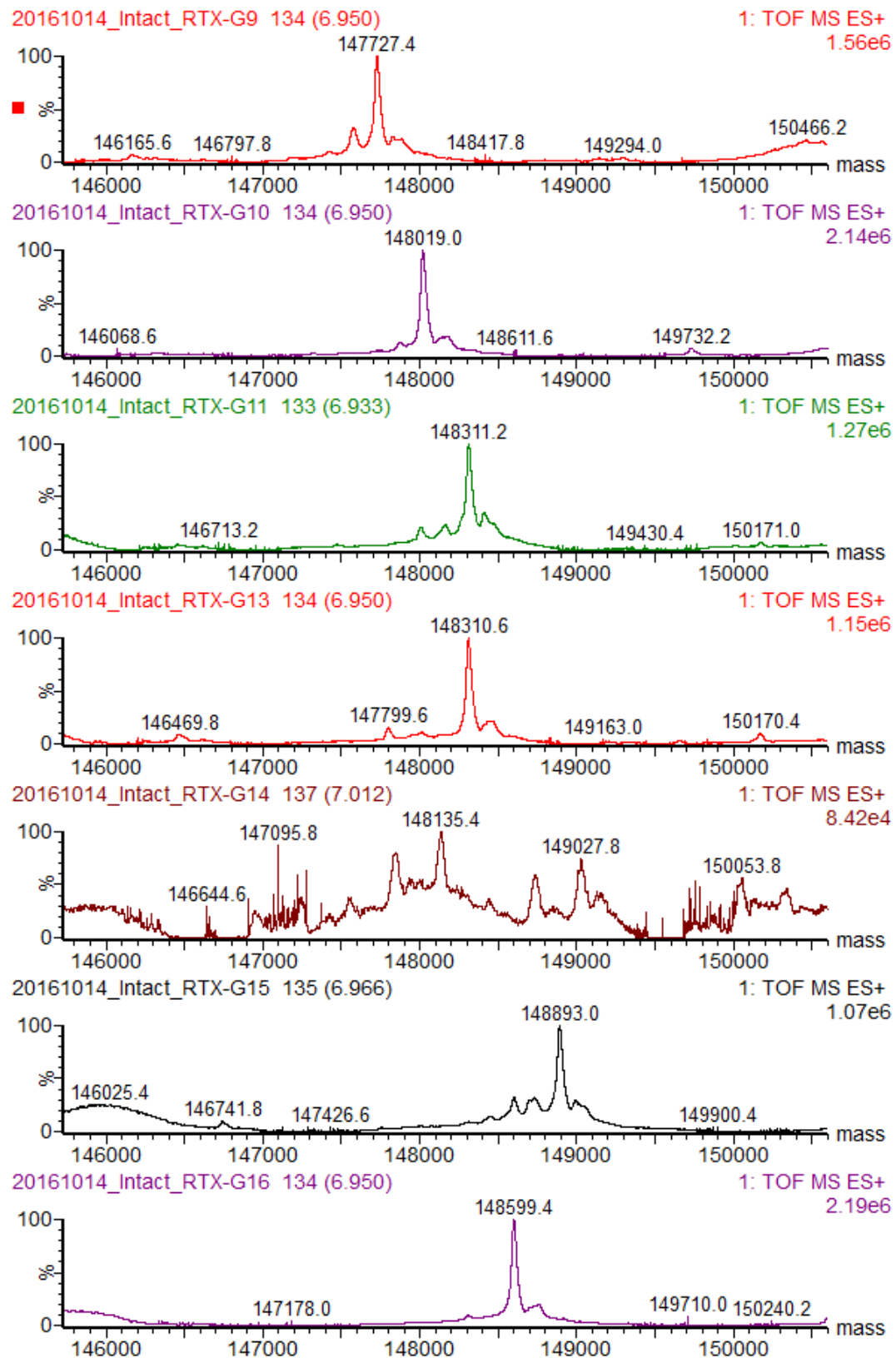


**Figure S11:** Intact mass analysis of glycoengineered antibodies (Rtx G9-G16)

## 9 Binding affinity of glycoengineered anti-CD20 antibodies to FcγRIIIA

The affinity of the remodeled glycoforms of Rituximab for FcγRIIIA receptors was examined by ELISA. Microtiter plate (Corning® 96 Well Clear Flat Bottom Polystyrene High Bind, #9018) was coated with 50 ng/well of recombinant soluble FcγRIIIA diluted in 50mM Bicarbonate/carbonate *coating buffer* (pH 10) overnight at 4°C. The plate was then washed 3 times with PBST (0.05% Tween 20 in PBS) and blocked with 5% BSA in PBST for 1 h at room temperature. The binding activity of glycoengineered antibodies (Rtx G1-G16) was determined for serial eight dilutions, starting with concentration of 100 µg/ml in 2% BSA/PBST in duplicates. The plate was incubated for 1 h at room temperature, and washed 3 times with PBST. Next, 100 µl of goat anti-human IgG conjugated to *horseradish peroxidase* (Jackson immune, #109-035-088) in 2% BSA/PBST was added per well and incubated for 30min at room temperature. The plate was washed 5 times with PBST then 100 µL per well of TMB substrate (eBioscience, #00-4201-56) was added and the resulting plate was incubated in the dark 15min at room temperature. The absorbance value was determined at 450 nm in an ELISA reader (Molecular Devices Corporation, Sunnyvale, CA, USA).

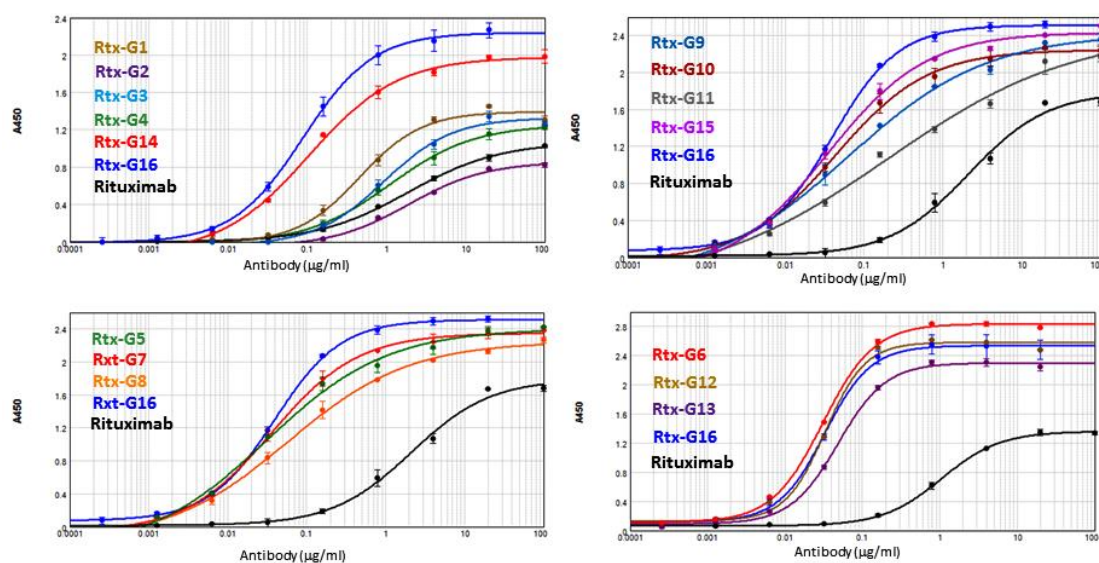


**Figure S12:** FcγRIIIA receptor bindings of commercial Rituximab and glycoengineered antibodies

**Table S4: Binding between FcγRIIIA and glycoengineered Rituximabs.**

Antibody	EC <sub>50</sub> , ng/mL <sup>[a]</sup>	Max. binding (A450 nm)	EC <sub>50</sub> Fold
Rtx-Commercial	1045	1.2	1
Rtx-G1	160	1.4	6.5
Rtx-G2	1050	1.1	~1
Rtx-G3	320	1.3	3.2
Rtx-G4	394	1.2	2.7
Rtx-G5	31	2.6	35
Rtx-G6	32	2.8	34
Rtx-G7	31	2.5	35
Rtx-G8	34	2.3	32
Rtx-G9	61	2.4	17
Rtx-G10	43	2.2	26
Rtx-G11	199	2.4	5.4
Rtx-G12	33	2.6	33
Rtx-G13	48	2.6	22
Rtx-G14	33	2.4	33
Rtx-G15	34	2.3	32
Rtx-G16	32	2.5	34

[a] EC<sub>50</sub> refers to the concentration of antibody that gives 50% of maximal binding

## 10 ADCC activity of glycoengineered anti-CD20 antibodies

The antibody-mediated ADCC was evaluated using the calcein release assay. Raji cells (human Burkitt's lymphoma cell line) were obtained from BCRC as target cells. Peripheral blood-mononuclear cells (PBMC) were separated from the blood of healthy volunteers using Ficoll-Paque (GE healthcare) as effector cells. The target cells ( $1 \times 10^6$  /ml) were labeled for 30 minutes at 37°C with 10 μM calcein-acetoxymethyl ester (Thermo Fisher Scientific). After washing, labeled target cells

were distributed in 96-well plates at a density of  $1 \times 10^4$  cells in 50  $\mu$ l per well. Antibodies with various concentrations, and effector cells ( $2.5 \times 10^5$  per well) with a 25:1 E/T ratio were then added. After incubation for 4h at 37 °C, cells were sedimented by centrifugation, and 150  $\mu$ l of supernatants were collected and analyzed by using fluorescence microplate reader to measure the release of calcein. For maximal release, the cells were lysed with 1% Triton X-100.

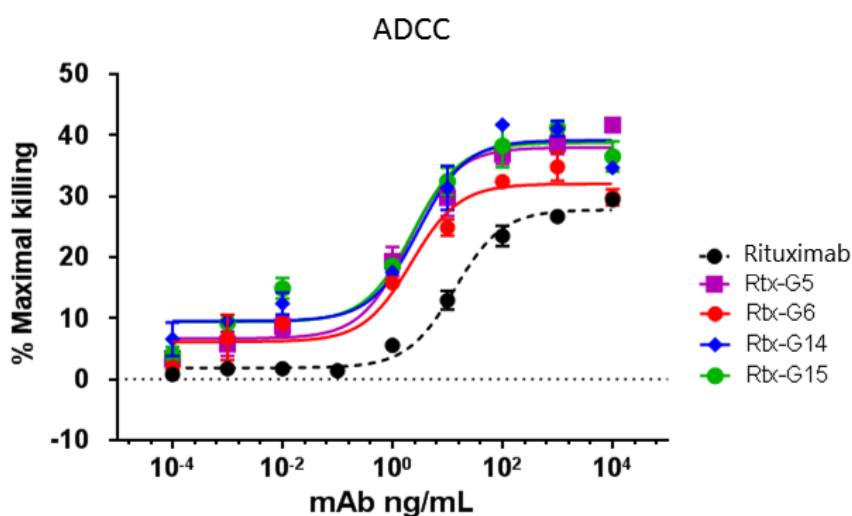


**Figure S13:** ADCC assays of glycoengineered anti-CD20 antibodies

**Table S5:** ADCC activities of selected glycoengineered Rituximab

Antibody	EC <sub>50</sub> <sup>[a]</sup> (ng/ml)	Maximum killing (%)	EC <sub>50</sub> Fold	Maxi killing fold
Rtx-G5	1.91	37.98	7.1	1.4
Rtx-G6	2.18	32.02	6.2	1.2
Rtx-G14	2.93	39.18	4.6	1.4
Rtx-G15	2.32	38.76	5.8	1.4
Rituximab	13.55	27.79	1.0	1.0

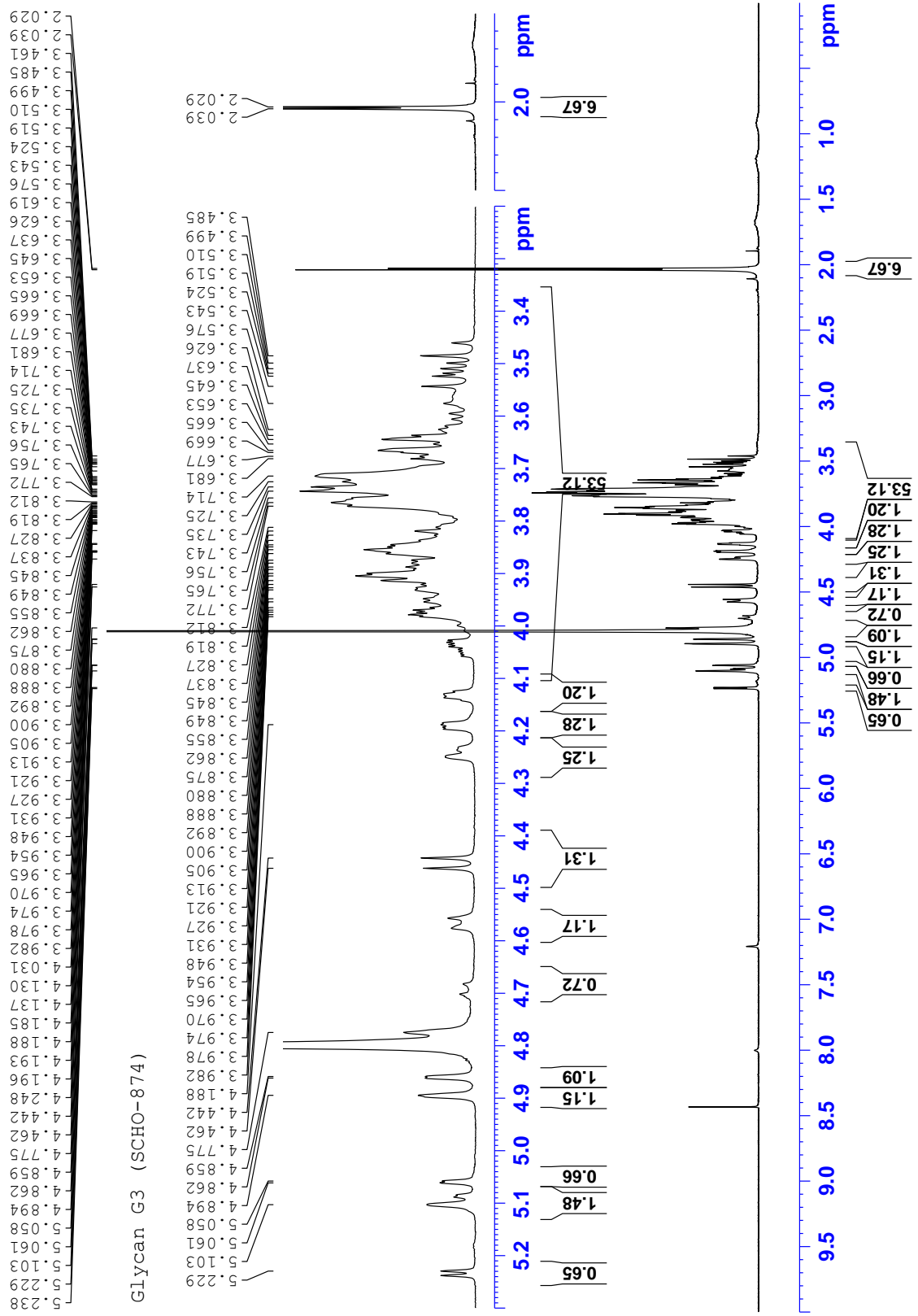
[a] EC<sub>50</sub> refers to the concentration of antibody that gives 50% of maximal cell killing

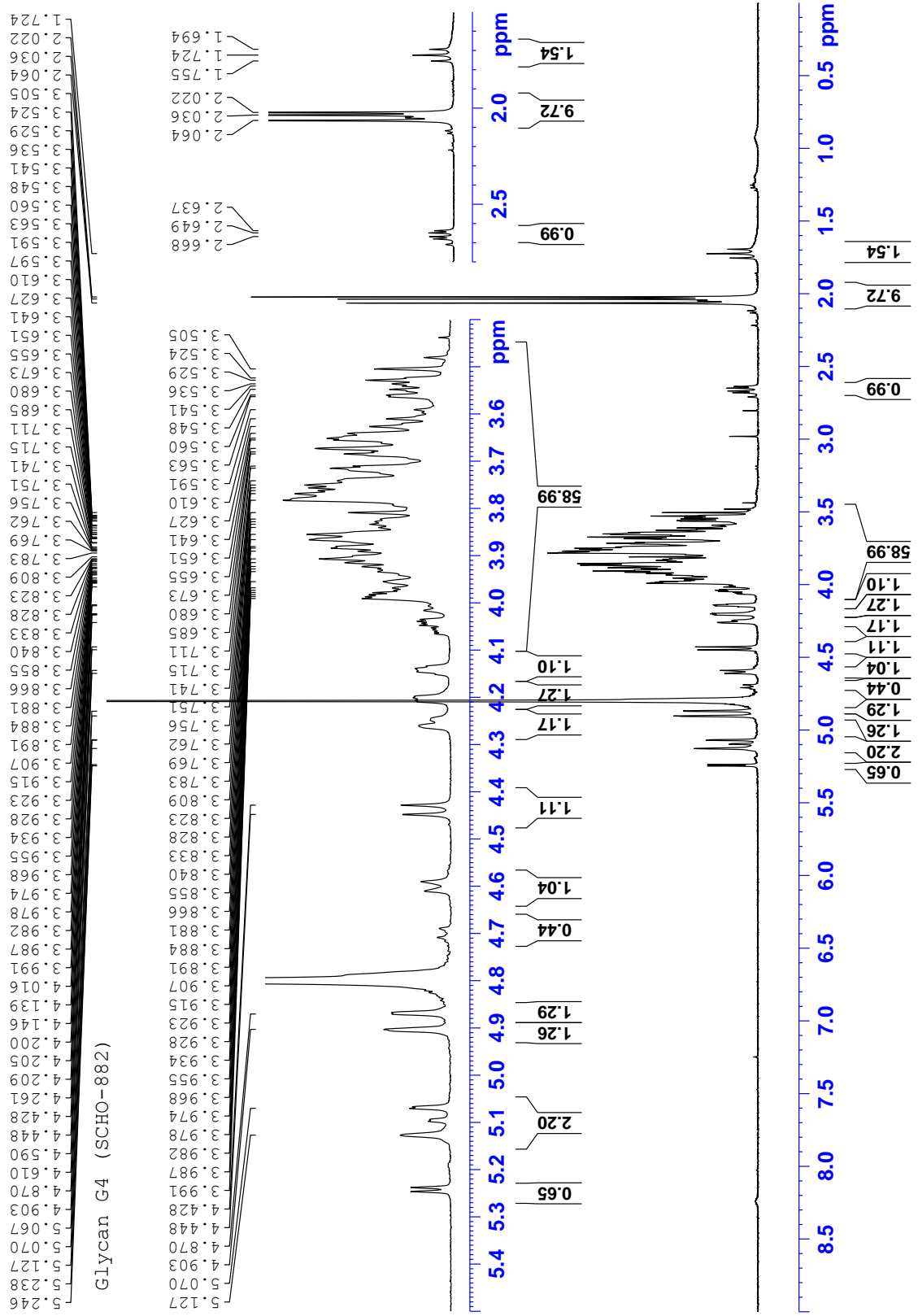
## 11 References:

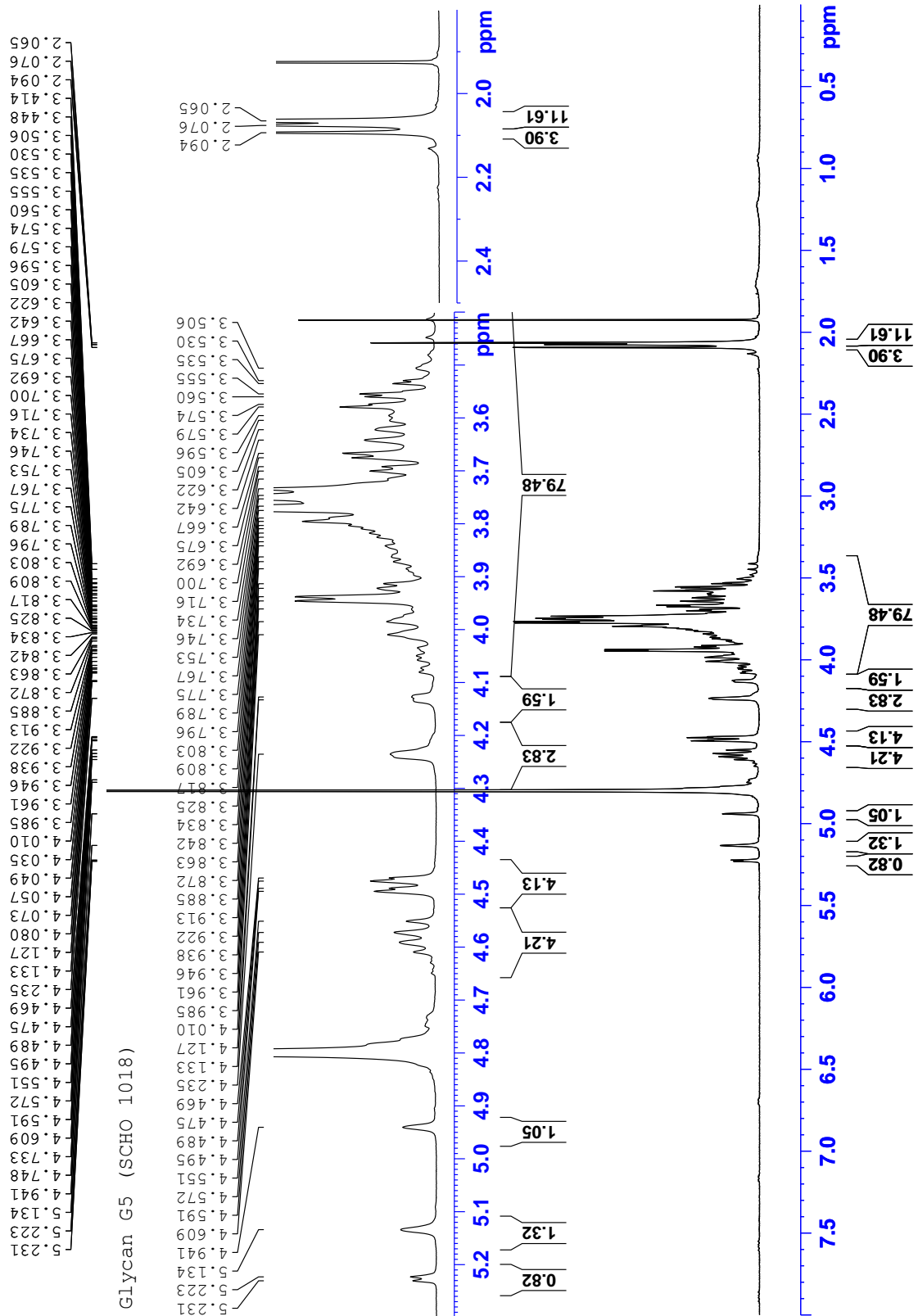
1. C. W. Lin, M. H. Tsai, S. T. Li, T. I. Tsai, K. C. Chu, Y. C. Liu, M. Y. Lai, C. Y. Wu, Y. C. Tseng, S. S. Shivatare, C. H. Wang, P. Chao, S. Y. Wang, H. W. Shih, Y. F. Zeng, T. H. You, J. Y. Liao, Y. C. Tu, Y. S. Lin, H. Y. Chuang, C. L. Chen, C. S. Tsai, C. C. Huang, N. H. Lin, C. Ma, C. Y. Wu, and C. H. Wong, *Proc. Natl. Acad. Sci. USA* 2015, **112**, 10611.
2. Y. Takakura, H. Tsukamoto and T. Yamamoto, *J. Biochem.* 2007, **142**, 403.
3. H. Tsukamoto, Y. Takakura, T. Mine and T. Yamamoto, *J. Biochem.* 2008, **143**, 187.
4. S. S. Shivatare, S. H. Chang, T. I. Tsai, C. T. Ren, H. Y. Chuang, L. Hsu, C. W. Lin, S. T. Li, C. Y. Wu and C. H. Wong, *J. Am. Chem. Soc.* 2013, **135**, 15382.
5. T. I. Tsai, H. Y. Lee, S. H. Chang, C. H. Wang, Y. C. Tu, Y. C. Lin, D. R. Hwang, C. Y. Wu and C. H. Wong, *J. Am. Chem. Soc.* 2013, **135**, 14831.
6. T. Li, X. Tong, Q. Yang, J. P. Giddens and L. X. Wang, *J. Biol. Chem.* 2016, **291**, 16508.

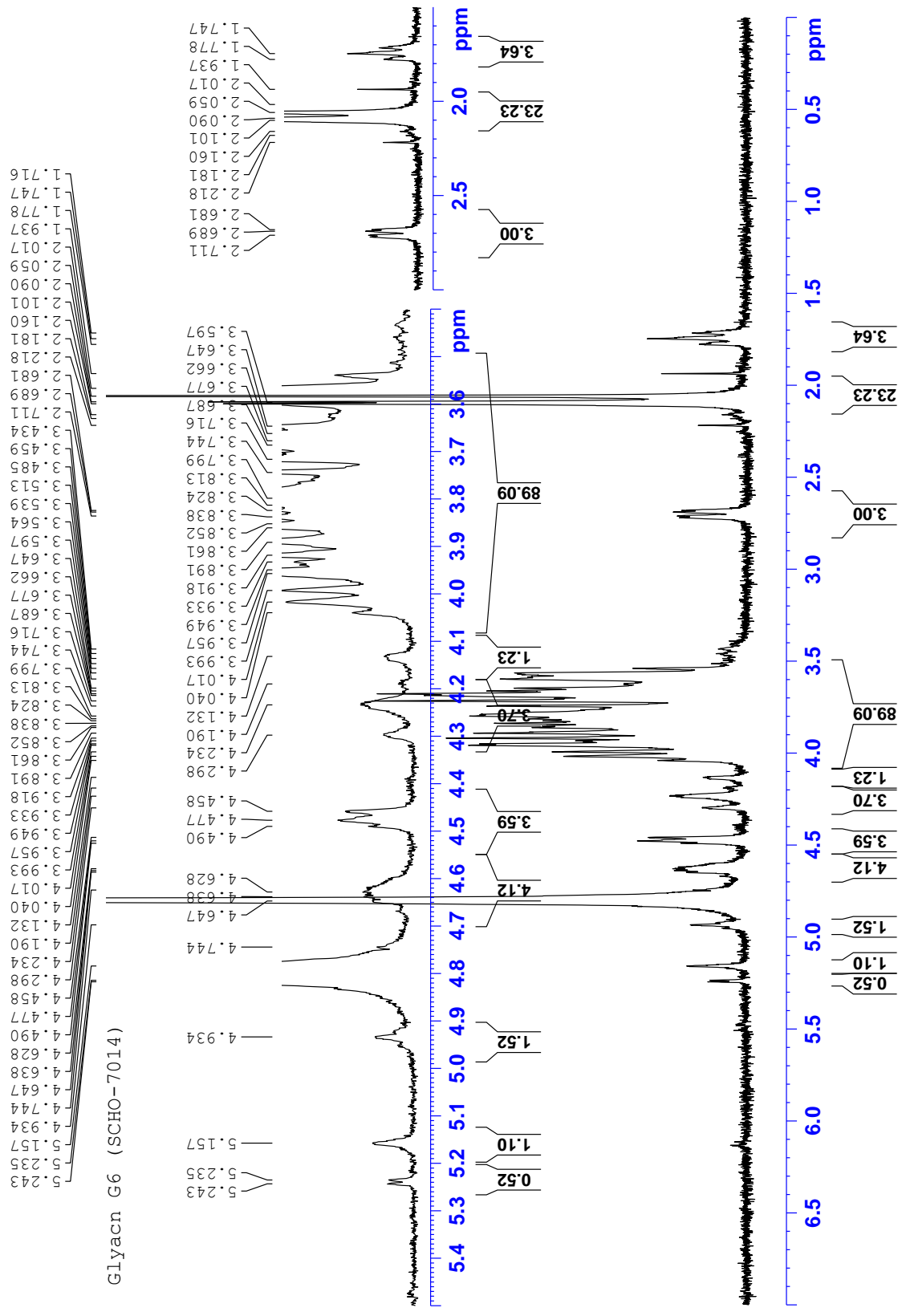






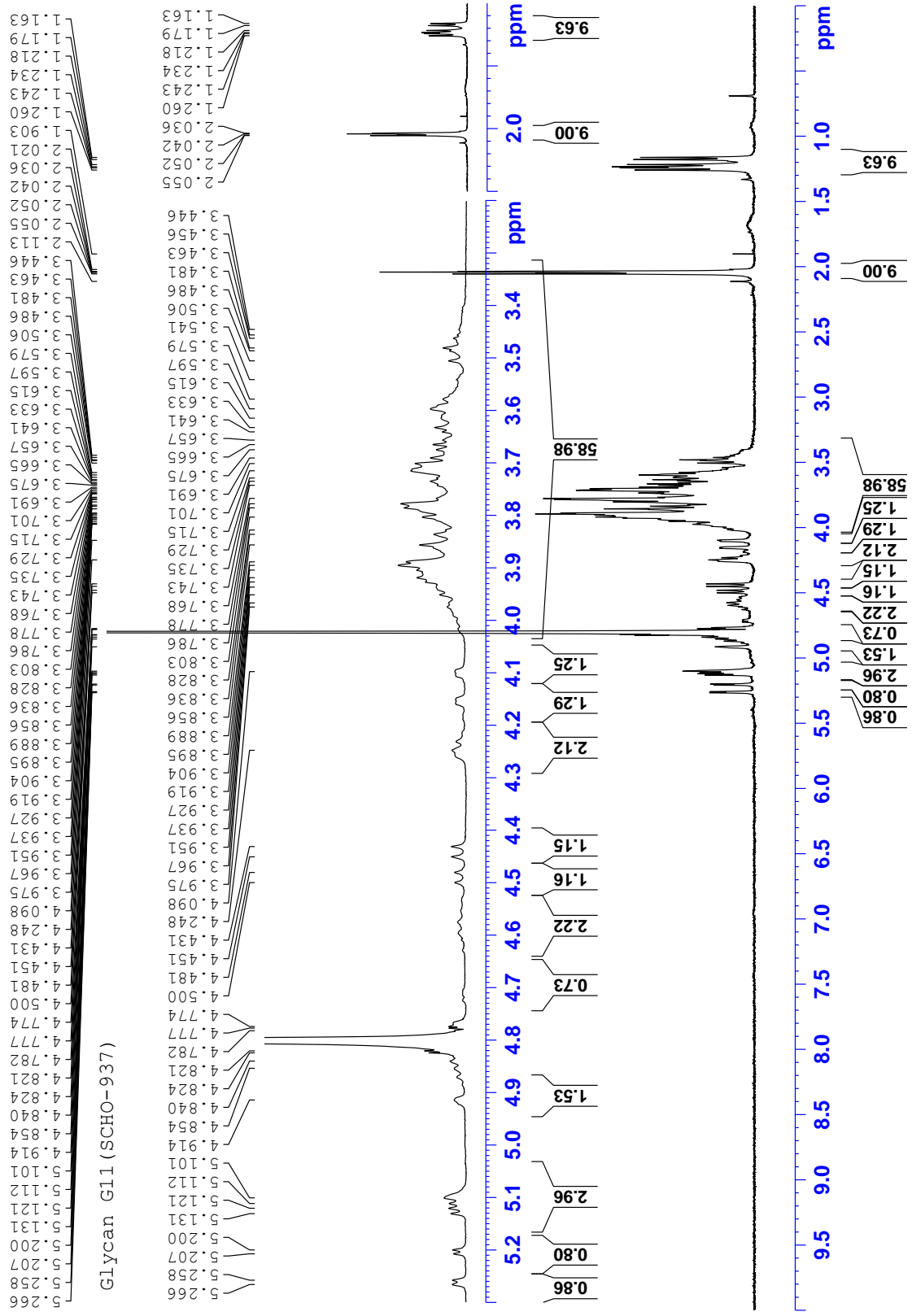


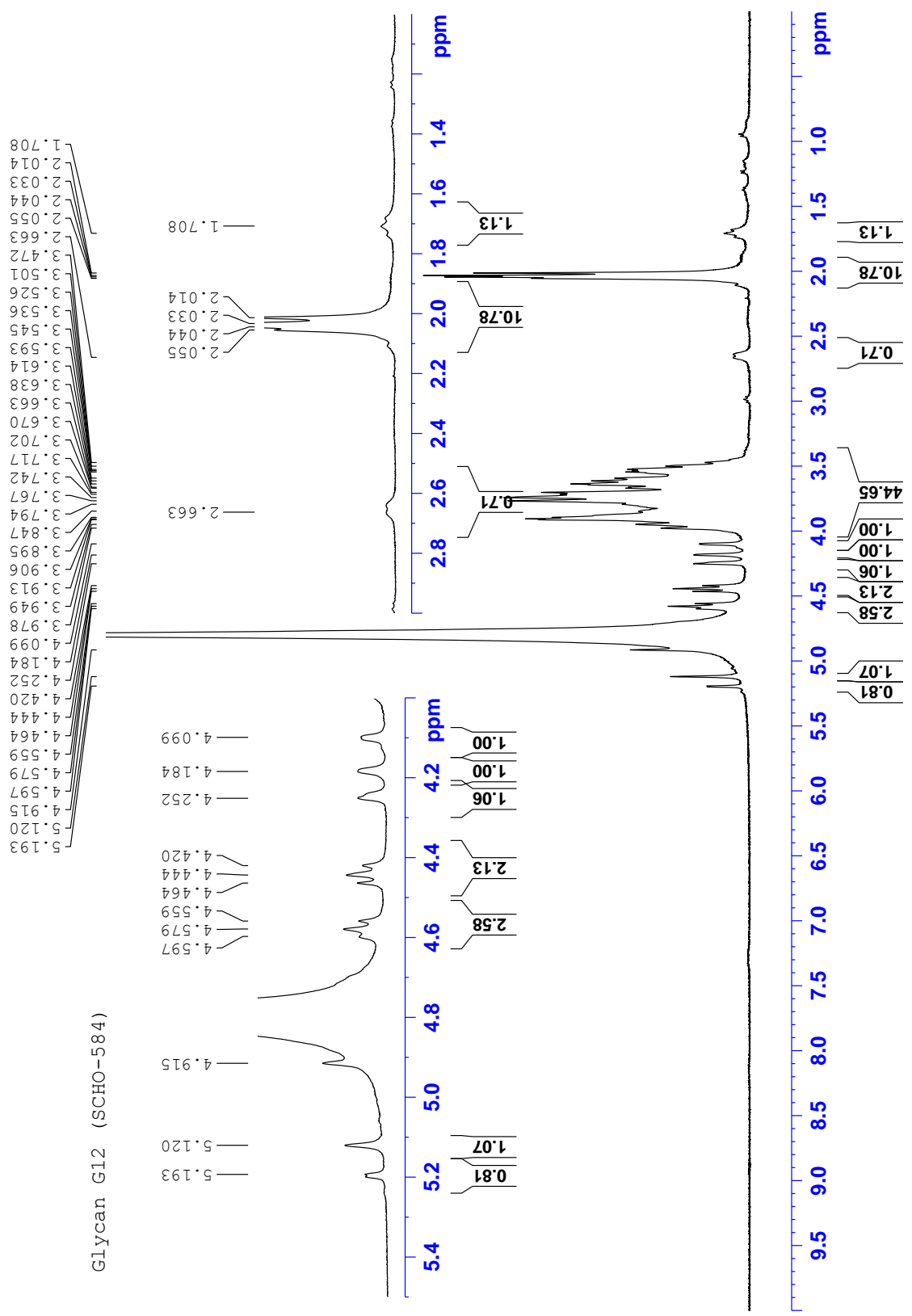












Glycan G13\_ (SCHO-589)

